Note: This is a preprint of paper being submitted for publication. Contents of this paper should not be quoted nor referred to without permission of the author(s).

Submitted to Symposium Q: Film Synthesis and Growth Using Energetic Beams
Materials Research Society Meeting
San Francisco Marriott, San Francisco, CA
April 17–21, 1995

AMORPHOUS DIAMOND-LIKE CARBON FILM GROWTH BY KrF- AND ArF-EXCIMER LASER PLD: CORRELATION WITH PLUME PROPERTIES

A. A. PURETZKY*, D. B. GEOHEGAN**, G. E. JELLISON Jr.**, AND
M. M. McGIBBON***
*Institute of Spectroscopy, Troitsk, Russia
**Oak Ridge National Laboratory, Oak Ridge, TN
***University of Glasgow, Glasgow, United Kingdom

April 1995

Prepared by
Solid State Division
Oak Ridge National Laboratory
P.O. Box 2008
Oak Ridge, Tennessee 37831-6056

managed by MARTIN MARIETTA ENERGY SYSTEMS, INC.
for the
U.S. DEPARTMENT OF ENERGY
under contract DE-AC05-84OR21400

DISCLAIMER

DISCLAIMER

Portions of this document may be illegible in electronic image products. Images are produced from the best available original document.

CONF-

AMORPHOUS DIAMOND-LIKE CARBON FILM GROWTH BY KrF- AND ArF-EXCIMER LASER PLD: CORRELATION WITH PLUME PROPERTIES

A. A. PURETZKY*, D. B. GEOHEGAN**, G. E. JELLISON Jr.**, AND
M. M. McGIBBON***
*Institute of Spectroscopy, Troitsk, Russia
**Oak Ridge National Laboratory, Oak Ridge, TN
***University of Glasgow, Glasgow, United Kingdom

ABSTRACT

A comparative study of ArF- and KrF-laser deposition of amorphous diamond-like carbon (DLC) films and relevant carbon plasmas has been performed. Spectroscopic ellipsometry and EELS analysis of the DLC films deposited on Si <100> and NaCl substrates were utilized to characterize the high quality ArF- and KrF-laser deposited films (up to 84% of sp^3 bonded carbon in 7 J/cm^2 -ArF-laser DLC film). Gated ICCD imaging, luminescence and ion current probe diagnostics of the carbon plume have revealed quite different properties of carbon plasmas generated by ArF- and KrF- lasers. KrF-laser (6.7 J/cm^2) irradiation produces a less energetic carbon plasma containing larger amounts of C_2 and probably larger clusters compared with ArF-laser irradiation at the same energy fluence. We conclude that the more energetic and highly-atomized ArF-laser carbon plasma results in the better diamond-like properties.

INTRODUCTION

Recently pulsed laser ablation of graphite with ultraviolet excimer laser wavelengths was found to permit the production of high quality amorphous diamond-like carbon (DLC) films.[1,2] Pulsed laser deposition (PLD) of carbon in high vacuum conditions with KrF- (248 nm) and ArF- (193 nm) lasers allows one to produce amorphous diamond like films with smooth (< 20 nm) surface morphology and high degree of diamond like character (large fraction of sp^3 bonded carbon). The important practical feature of the UV excimer PLD process is that much lower laser energy fluences (5–20 J/cm^2) are required compared to visible and IR laser PLD processing.[2]

In this work a comparative study of ArF- (193 nm) and KrF (248 nm) laser deposited diamond-like films has been performed and correlated with gated-ICCD imaging, optical spectroscopic and ion current probe diagnostics of the corresponding laser-generated carbon plasmas. Higher quality DLC films were obtained using ArF-laser irradiation compared to KrF-laser PLD, as determined by EELS and spectroscopic ellipsometry analysis. The plasma diagnostics revealed several key differences between the plasmas generated by these two lasers. ArF-laser (6.7 J/cm^2) generated plasma consisted of a fast propagating ball-shaped component of luminescence containing highly excited C^{++}, C^+, and C species followed by a slower component of cooler, atomized material (C, C^+), followed by a third component which appears to contain C_2, clusters and ultrafine particles. At the same fluence, the KrF-laser does not produce a luminescent plasma ball and appears to produce larger amount of luminescent C_2 and heavier clusters and ultrafine particles at later times after the laser pulse. The higher quality DLC films obtained with 193-nm ArF-laser irradiation appears correlated with both the smaller amount of clusters and ultrafine particles as well as with the higher kinetic energies of carbon ions and atoms generated by this laser.

EXPERIMENTAL

The experimental set up has been described previously.[3,4] It consists of a stainless steel high vacuum chamber (40 cm diameter) equipped with Suprasil quartz windows for optical diagnostics. The chamber is pumped by a turbomolecular pump to a base pressure of 5×10^{-7} Torr. A Questek

(Model 2960) excimer laser operating on ArF (22 ns FWHM, 600 mJ) or KrF (28 ns FWHM, 900 mJ) was used. The beam was apertured and focused into the chamber with a spherical lens (500 mm f.l. at 248 nm, 445 mm f.l. at 193nm) to a rectangular beam spot (0.18 cm × 0.11 cm) at an incidence angle of 30° onto 1"-diameter pyrolytic graphite pellets (Specialty Minerals Inc., less than 10 ppm total impurities). The pellets were rotated during the film deposition and plasma plume diagnostics experiments. The maximum laser fluences at the pellet surface were 7 J/cm^2 (ArF) and 20 J/cm^2 (KrF). N-type Si (100) wafers (resistivity 0.2–0.4 ohm-cm) were used as substrates for PLD. The substrates were kept at room temperature and placed at variable distances from the target (d = 4-15 cm). NaCl crystals were also used as substrates for films deposited especially for EELS analysis.

Films were characterized by transmission electron microscopy (STEM), electron energy loss spectroscopy (EELS) and spectroscopic ellipsometry.

Gated imaging was done with an intensified charge-coupled device (ICCD), lens-coupled camera system (Princeton Instruments) with variable gain and gate width (5-ns minimum) and a spectral range from 200-820 nm.

Spectroscopic measurement of the plume luminescence was performed with a 1.33-meter spectrometer (McPherson 209) equipped with an 1800 g/mm holographic grating, an intensified, gated diode array (Princeton Instruments IRY-700RB) and a photomultiplier tube (Hamamatsu R955).

FILMS CHARACTERIZATION

The fraction of sp^3-bonded carbon in the films was estimated using the EELS spectra. The spectra were obtained with a VG HB501 UX dedicated scanning transmission electron microscope (STEM) operated at an accelerating voltage of 100 KeV.[5] The 30 nm-thick DLC films for EELS analysis were deposited on NaCl-substrates using ArF-laser irradiation (11.1 Hz repetition rate, 4660 pulses, 5.6 cm substrate-target distance). The substrate was then dissolved in deionized water and the DLC-film was put on the STEM specimen copper grid. In order to estimate the fraction of sp^3 bonded carbon, the EELS spectrum of crystalline carbon was measured as well. Figure 1(a) and 1(b) shows carbon K-edge spectra of an amorphous diamond-like carbon film (a) and a crystalline graphite film (b) after subtraction of background.

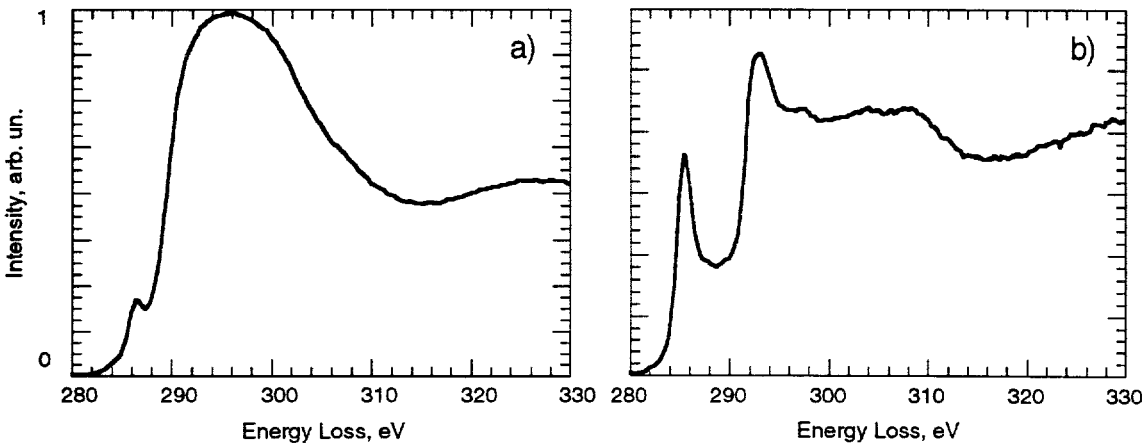

Fig. 1 (a) EELS spectrum of ArF-laser deposited DLC film (NaCl substrate dissolved) in the carbon K-edge core-loss region. (b) EELS spectrum of graphitized carbon, for comparison.

The peak at 285.5 eV [Fig. 1(b)] corresponds to transitions from 1s to π^*. The 1s-σ^* transition is responsible for the higher energy peaks. In the amorphous DLC film the 1s-π^* peak (286.6 eV) is much smaller than that for the graphitized carbon sample due to the small amount of sp^2-bonded carbon in the DLC film. The 1s-σ^* peaks (>290 eV) in DLC films are broader

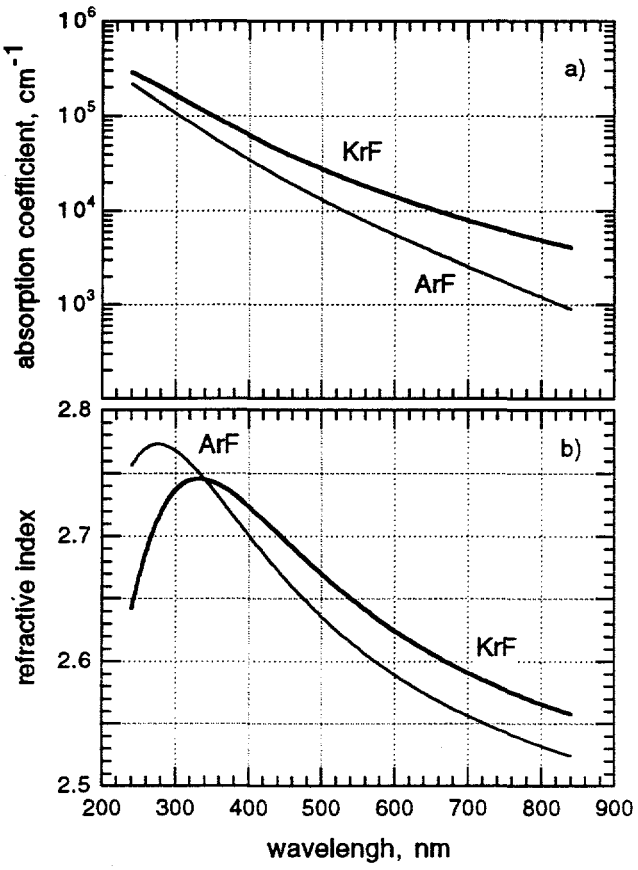

Fig. 2 (a) Absorption coefficient and (b) refractive index versus wavelength for ArF- (7.0 J/cm^2, 11 Hz repetition rate, 3.0x10^4 pulses) and KrF- (16.7 J/cm^2, 11 Hz repetition rate, 2.4 x 10^4 pulses) laser-deposited DLC films. The pellet-substrate distance was 9 cm.

compared to those in crystalline carbon because of the loss of structural order in the amorphous material. The $sp^3/(sp^3+sp^2)$ ratio was estimated by the standard procedure[6] and found to be about 84% for this ArF-laser deposited film (on NaCl-substrate). The low energy spectra also clearly demonstrated the amorphous diamond-like character of the deposited films, i. e., the 26 eV-plasmon peak was shifted to 30 eV and the 6.7 eV- π-π^* antibonding transition could not be resolved because of the very low fraction of sp^2 bonded carbon.

The optical properties of both ArF- and KrF-laser deposited films were measured by spectroscopic ellipsometry. These measurements were performed on a two-channel polarization modulation ellipsometer[7] which measures the three associated ellipsometric parameters, N=cos2ψ, S=sin2ψsinΔ and C=sin2ψcosΔ (ψ and Δ are the ellipsometric angles) simultaneously in a single scan. The spectral range investigated was 240–840 nm. The real and imaginary parts of the complex refractive index were obtained by fitting the experimental curves using a five-parameter model developed by Forouhi and Bloomer for amorphous semiconductors[8] (for details see Ref. 9). Two films, one deposited by KrF-laser and one by ArF-laser, were analyzed. For the KrF-laser film (380 nm maximum thickness measured by profilometry), the best fit (χ^2=0.7) to the experimental data was obtained with the following sequence of layers: (1) rough layer (0.74-nm), (2) DLC film (327.1 nm), (3) interface layer (14.5 nm), and finally c-Si. The same layer model applied to the ArF-laser generated film (127 nm maximum thickness measured by profilometry) also gave a good fit to experimental data (χ^2=2.6). The derived thicknesses of the layers are: (1) 0.98 nm, (2) 110.4 nm and (3) 3.9 nm, respectively (see above). Figure 2(a)and 2(b) compare the wavelength dependence of the absorption coefficient and the refractive index for ArF- and KrF-laser deposited DLC films.

The **n** values measured for this films changed from 2.56 to 2.74 (KrF) and 2.52 to 2.77 (ArF) in the spectral range studied. By comparison, the n value for diamond varies from 2.40 to 2.66 over the same spectral region. The lower absorption coefficient for the ArF-laser DLC (versus the KrF-laser film) corresponds with the trend noted during the entire series of runs, i.e., (a) higher electrical resistance and (b) more transparent diamond-like films are obtained with the ArF-laser compared to those deposited using the KrF-laser. It should be emphasized that the higher-quality ArF-laser DLC of Fig. 2 was achieved with nearly 3-times less laser power compared to that used with the KrF-laser, despite the general trend of higher quality DLC material with increasing laser energy for both wavelengths. The ellipsometry data also indicate substantial differences between the interfacial layer properties for these two cases. The refractive indices of ArF- and KrF-laser produced interfacial layers differ greatly (n=3 and 2.4 at 2 eV, respectively).

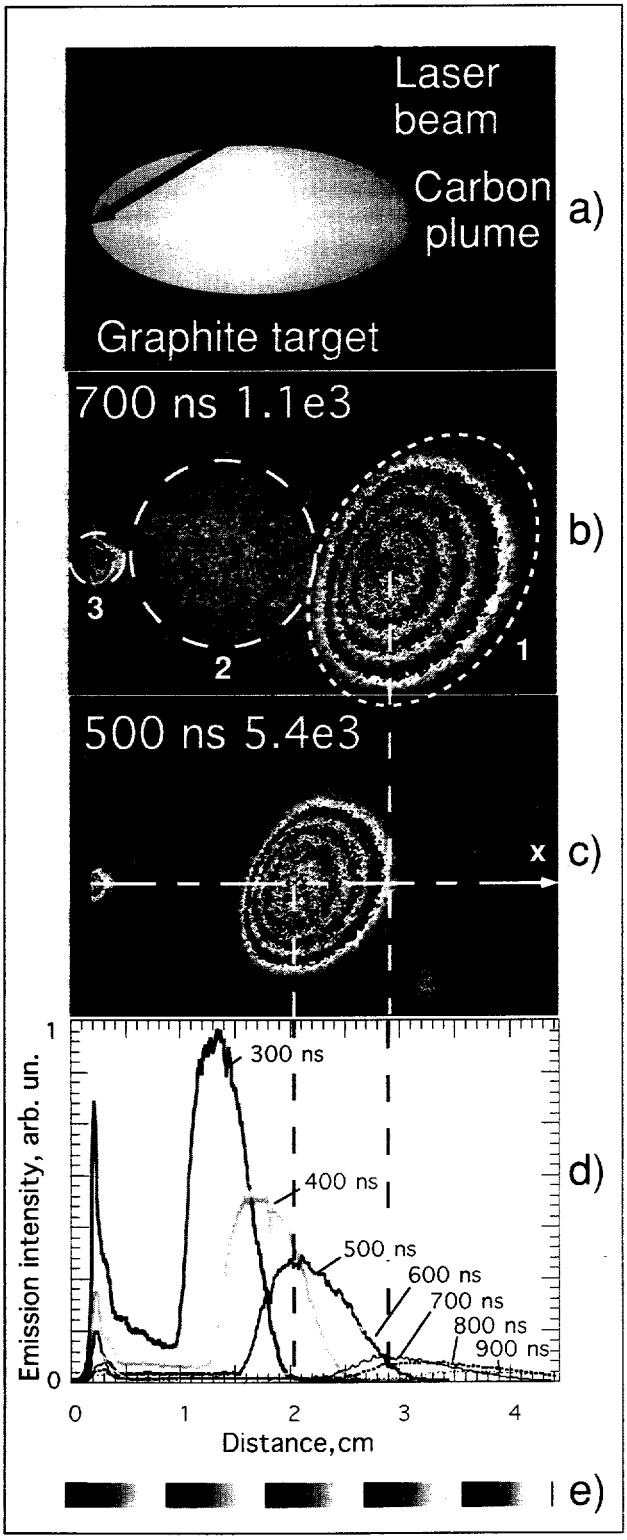

Fig. 3. (a) Irradiation geometry. (b),(c) Gated-ICCD photographs (5 ns gate width) of the total visible carbon plasma emission at (b) Δt = 700 ns and (c) 500 ns generated by ArF-laser (6.7 J/cm^2). Three distinct spatial regions are indicated in (b) (see text). The 5-grayscale palette is normalized to 1100 counts in (b) and 540 counts in (c). (d) A line-profile of the emission intensity from the irradiated spot along the target normal, **x**, shows the correct relative scaling between the emission intensities at different times (from 300 ns to 900 ns) .

CARBON PLUME DIAGNOSTICS

To understand the difference noted between the ArF- and KrF-laser deposited DLC films, in situ diagnostics of the carbon plasma plume were performed under the respective film growth conditions. Figure 3 show typical gated-ICCD images of the ArF-laser generated plume. Three well-separated regions within the ArF-laser generated carbon plume were discovered.

The first region noted [denoted 1 in Fig. 3 (b)] has the highest emission intensity and a characteristic ellipsoidal-ball shape. This plasma ball propagates with the average velocity v_{pr} about 3.9 cm/μs, estimated from the propagation of the emission maximum. This region expands as well with a characteristic velocity of v_{exp} = 2.6 cm/μs. The second region [2 in Fig. 3(b)] is characteristically round, and it also propagates and expands. The maximum of emission intensity within this region propagates with decreasing average velocity which changes from 1.2 cm/μs (700 ns image) to 0.7 cm/μs (3 μs image, not shown). The third region [3 in Fig.3 (b)] is characterized by relatively intense emission and propagates with a much smaller velocity of only about 0.1 cm/μs.

To clarify what species are responsible for the observed emission, luminescence spectroscopy was performed at different distances from the target surface as well as ion probe current measurements and filtered ICCD-imaging in particular spectral regions corresponding to C^+, C, and C_2. Figure 4 (a),(b) shows representative luminescence waveforms observed for C^+ and C at 2.15 cm (a) and 4.0 cm from the target surface.

A comparison of the total emission measured by imaging with the luminescence profiles [Fig. 4(a)] indicates that predominantly C^+ and C species are responsible for the bright emission in the first region. Neutral C luminescence has two characteristic components. As shown in Fig. 4(a),

the first occurs during the C^+ luminescence [Fig. 4 (a)] while the second component luminescence (maximum at 0.8 μs) lasts about 2 μs and is correlated with the second imaged region.

At smaller distances from graphite target (d < 1.0 cm) C^{++} luminescence (λ=229.7 nm, from 145 875 cm^{-1}) was also detected. The peak C^{++} emission corresponded with that of C^+ at these distances, and the first component of C emission. One can conclude from these data that the fast propagating ball (Figs. 3(b)–3(d) is a propagating and recombining carbon plasma containing electronically excited species of C^{++}, C^+, and C. Continual recombination results in the appearance of fast neutrals which appears as the first component of the C– luminescence waveform [Fig. 4(a)]. Recombination also maintains the electron temperature within the plasma ball, slowing the drop of T_e during the plasma expansion.

A comparison of the ion current and C^+ emission time profiles in Fig. 4(b) indicate that, in addition to the luminescent C-neutrals, non-emitting ground state ions are also present within the second ball of emission. Region 3 emission was attributed principally to C_2 luminescence from gated-ICCD images of the C_2 Swan bandheads using 515.5 nm and 560.0 nm (10 nm bandwidth, FWHM) filters (not shown).

A comparison between ArF- and KrF-laser generated plasma plumes is given in Fig. 5 at 1μs after the laser pulse. Two notable differences are found. First, the KrF-laser carbon plasma generated at the same fluence (6.7 J/cm^2) does not show a fast-propagating plasma ball [region 1 in Fig. 3 (b)], although the region-2 luminescence is present. To generate the fast plasma ball the KrF-laser fluence needs to be increased to approximately 17 J/cm^2 [see Fig. 5(c)]. However, in this case intense C_2 emission is also observed.

The second main difference between ArF and KrF-generated plasma plumes is the production of many more luminescent C_2 and possibly higher-mass clusters for KrF, as can be seen clearly by comparing the third region luminescence in Figs. 5(a)-5(c).

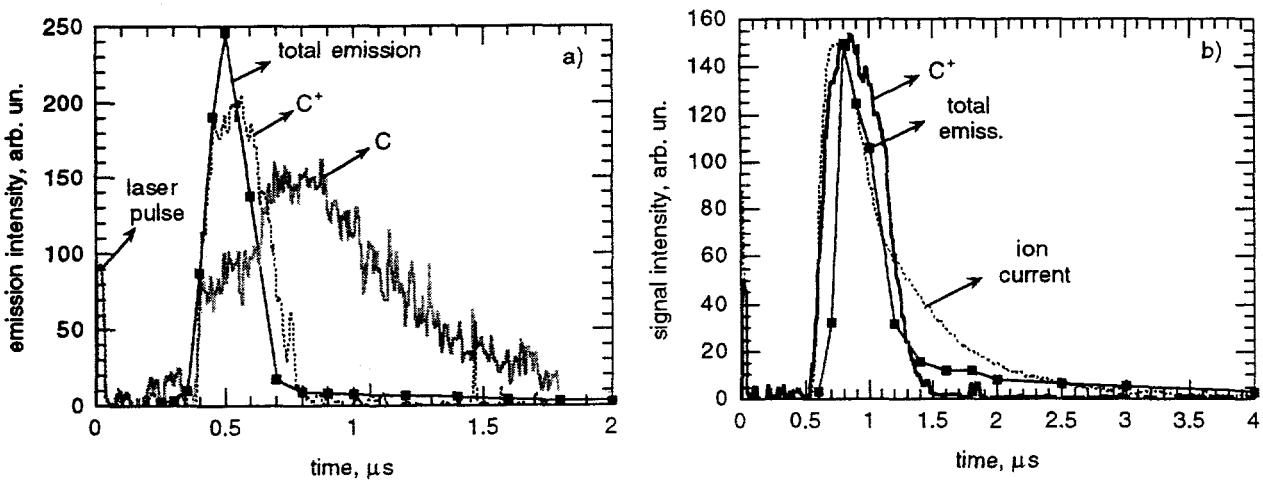

Fig. 4 ArF-laser, (6.7 J/cm^2) generated (a) Luminescence of C^+ (λ=426.7 nm, originating from 168979 cm^{-1} above ground) and C (λ=247.9 nm, 61982 cm^{-1} above ground) and the total emission calculated from the set of ICCD imaging spatial intensity line-profiles (from Fig. 3(d) at d = 2.15 cm from the target surface) . (b) Luminescence, total emission and ion current (peak current 0.3 A) waveforms normalized to their maximum values measured at 4.0 cm from the target surface . The ion probe was biased to -70 V (floating with respect to its shield).

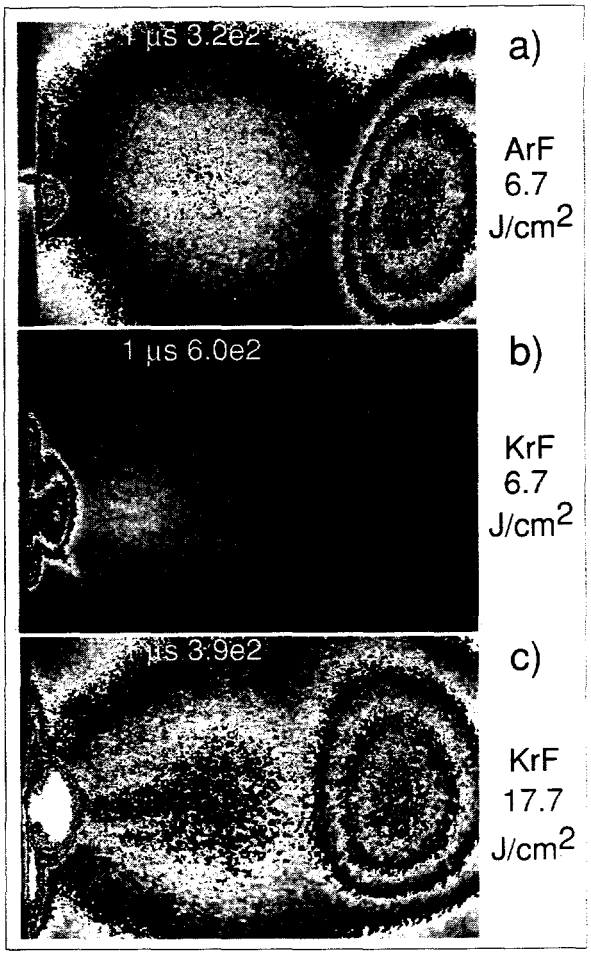

Fig. 5 Gated ICCD images of ArF- (a) (6.7 J/cm^2) and (b,c) KrF- (6.7 J/cm^2 and 17.7 J/cm^2, respectively) laser generated plasmas at 1 µs after the laser pulse. The 5-grayscale palette [Fig.3(e)] is normalized to (a) 320 counts , (b) 600 counts and (c) 390 counts (equal exposures, 50 ns gates).

CONCLUSION

A comparative study of ArF- and KrF-laser deposited amorphous diamond like carbon (DLC) films has been performed in conjunction with relevant plasma diagnostics of the plasma plumes. ArF-laser irradiation produces the highest quality amorphous DLC films, with higher optical transmission, higher index of refraction, better electrical insulation, and higher sp^3: sp^2 ratios than KrF-laser deposited DLC films. ArF-laser deposited films on NaCl substrates were estimated to contain 84% sp^3-bonded carbon. Unfiltered and species-resolved gated-ICCD imaging, spectroscopic, and ion probe current measurements show that the KrF-laser generates substantially larger amounts of ultrafine particles and C_2 (and probably larger clusters) compared to that generated with the ArF-laser. In addition, the KrF-laser generated plume at comparable fluences lacks the fast-propagating plasma ball noted using ArF irradiation. The KrF fluence must be increased to at least 17 J/cm^2 to generate the similar fast component. However, spectroscopic ellipsometric analysis shows that the ArF (7 J/cm^2) DLC films are still superior to the high-fluence KrF (17 J/cm^2) DLC films

The authors gratefully acknowledge many helpful discussions with S.J. Pennycook and D. H. Lowndes. This work was supported by the Division of Material Sciences, U.S. Department of Energy under contract DE-AC05-84OR21400 with Martin Marietta Energy Systems, Inc., and NIS/ IPP program sponsored by Division of Defense Programs, U.S. Departement of Energy under contract DP-15.

REFERENCES

1. D. L. Pappas, K. L. Saenger, J. Bruley, W. Krakov, J. J. Cuomo and R. W. Collins, *J. Appl. Phys.* **71**, 5675 (1992).
2. F.Xiong, Y. Y. wang, V. Leppert, R. P. H. Chang, *J. Mater. Res.* **8**, 2265 (1993).
3. D. B. Geohegan, *Thin Solid Films* **220**,138 (1992).
4. D. B. Geohegan, *Appl. Phys. Lett.* **60**, 2732 (1992).
5. N. D. Browning and S. J. Pennycook, *Microbeam Analysis* **2**, 81 (1993).
6. S. D. Berger, D. R. McKenzie, P. J. Martin, *Philosophical Magazine Letters* **57**, 285 (1988).
7. G. E. Jellison, Jr. and F. A. Modine, *Appl. Optics* **29**, 959 (1990).
8. A. R. Forouhi and I. Bloomer, *Phys. Rev. B* **34**, 7018 (1986).
9. G. E. Jellison, Jr., *Thin Solid Films* **234**, 416 (1993).
10. D. F. Edwards and H. R. Philipp, *Handbook of Optical Constants of Solids*, ed. by E. D. Palic, Academic Press, San-Diego, 1985, p.665.